# Synthesis and Properties of Au Hydride

Sil Devika, Lane Christopher, Glor Ethan, Gilroy Kyle D.,Sylla Safiya, Barbiellini Bernardo, Markiewicz Robert, Hajfathalian Maryam, Neretina Svetlana, Bansil Arun, Zahra Fakhraai Zahra, Borguet Eric

# Synthesis and Properties of Au Hydride

Dr. Devika Sil,†[1] Christopher Lane,†[2] Dr. Ethan Glor,†[3] Dr. Kyle D. Gilroy,[4,5] Safiya Sylla,[1] Prof. Bernardo Barbiellini,[6,2] Prof. Robert Markiewicz,[2] Dr. Maryam Hajfathalian,[5] Prof. Svetlana Neretina,[7] Prof. Arun Bansil,[2] Prof. Zahra Fakhraai,[3] and Prof. Eric Borguet*[1]

[1] *Department of Chemistry, Temple University, Philadelphia, Pennsylvania 19122, USA.*
[2] *Northeastern University Physics Department, 360 Huntington Ave.*
*111 Dana Research Center, Boston, MA 02115, USA.*
[3] *Department of Chemistry, University of Pennsylvania, 231 S. 34th Street, Philadelphia, PA 19104, USA.*
[4] *The Wallace H. Coulter Department of Biomedical Engineering, Georgia Institute of Technology and Emory University, Atlanta, GA 30332, USA.*
[5] *College of Engineering, Temple University, Philadelphia, PA 19122, USA*
[6] *Department of Physics, School of Engineering Science, LUT University, FI-53851 Lappeenranta, Finland*
[7] *College of Engineering, University of Notre Dame, Notre Dame, IN 46556, USA*


†These authors contributed equally to this work

*to whom correspondence should be addressed: eborguet@temple.edu

## Abstract

**The generation of chemical species from gases, noble metals and light interacting with localized surface plasmons represents a new paradigm for achieving low energy sustainable reaction pathways. Here, we demonstrate that the dissociation reaction of $H_2$ meditated by the decay of localized surface plasmons of gold nanoparticles leads to the generation of a new material as detected by a change in the optical properties of the gold nanostructures. The effective permittivity measured by in situ spectroscopic ellipsometry shows a blue-shift of 0.02 eV in the surface plasmon resonance, demonstrating the plausible formation of a metastable gold hydride layer on the surface of nanoparticles following the dissociation of $H_2$. The formation of this gold hydride through the interaction of gold with atomic H is supported by first-principles simulations. These calculations do not indicate a significant charge transfer upon hydrogenation of the (111) surface but rather large Friedel charge oscillations within the gold layer. Moreover, our blue-shift is produced by the formation of a hydride leading to changes in critical band gaps in the electronic structure. For a coverage of 11%, the calculated peak of the imaginary part of the ZZ-component of the dielectric tensor undergoes a blue shift of 28 nm from a hydrogen free peak at 574 nm.**

## Introduction

The interaction of gold with hydrogen, especially the formation of Au-H bonds, remains poorly understood due to the inert nature of bulk gold. According to Mukherjee *et al.*[1] thermodynamics alone cannot drive the dissociation of $H_2$ given the large activation energy of 4.51 eV. Therefore pathways to gold-hydride formation remain elusive, except possibly in some extreme conditions[2,3]. The interaction of noble metals with photons whose energy is in

resonance with the surface plasmons leads to the generation of hot electrons that can drive chemical reactions with a relatively low energy cost. In fact, unlike experimental methods of high-pressure and high-temperature synthesis of metal hydrides[3], plasmon driven syntheses operate under gentle ambient conditions. Clearly, noble metal nanoparticles can trigger reactions in which they provide both hot electrons via the localized surface plasmon resonance and the active site for photocatalysis[4]. These systems are being deployed in an increasing number of research fields including water splitting[5,6], solar energy harvesting[7], sensing[8,9], catalysis[1,10,11], generation of $H_2$ from alcohol[12], hydrocarbon conversion[13], fabrication of novel molecular electronic devices[14], plasmonic switches[15], quantum-dot plasmonic hybrid systems[16–18] and nanoscale electronics[19].

Mukherjee *et al.*[1] provided the first experimental evidence for the room-temperature photocatalytic dissociation of $H_2$ on gold nanoparticles using visible light by observing the production of HD from a mixture of $H_2$ and $D_2$. They inferred that a fraction of the hot electrons, generated by the resonantly excited gold nanoparticles, transfer into the antibonding orbitals of a physisorbed $H_2$ molecule, which then leads to the dissociation of the $H_2$ molecule. Mukherjee *et al.*[1] thus showed that the localized surface plasmon resonance in gold can dissociate $H_2$ without the need for an active material such as Pd. Sil *et al.*[20] leveraged this dissociation process to develop an all optical $H_2$ sensing scheme by exploiting shifts in the dielectric function of gold nanoparticle thin films upon adsorption of hydrogen[21]. Related studies have observed similar shifts, however there is no consensus on the direction of the shift, blue or red. In this study, we show how the formation of a metastable gold hydride layer hypothesized by Sil *et al.*[20], Silverwood *et al.*[22], Whittaker *et al.*[23] and Ishida et al.[24,25], following $H_2$ dissociation, explains the blue shift in the dielectric function of the gold-nanoparticle surface. *In situ* spectroscopic

ellipsometry combined with state-of-the-art density functional theory (DFT) based first-principles computations justify our proposed mechanism based on gold hydride formation and elicit unique insights into the interaction of gold nanoparticles with atomic hydrogen.

## Results and discussion

Measurements were performed using spectroscopic ellipsometry to investigate the effect of hydrogen on the dielectric function of dewetted gold nanoparticle thin film samples on microscope glass slides under broadband illumination. Sample preparation details are given in the Methods section.
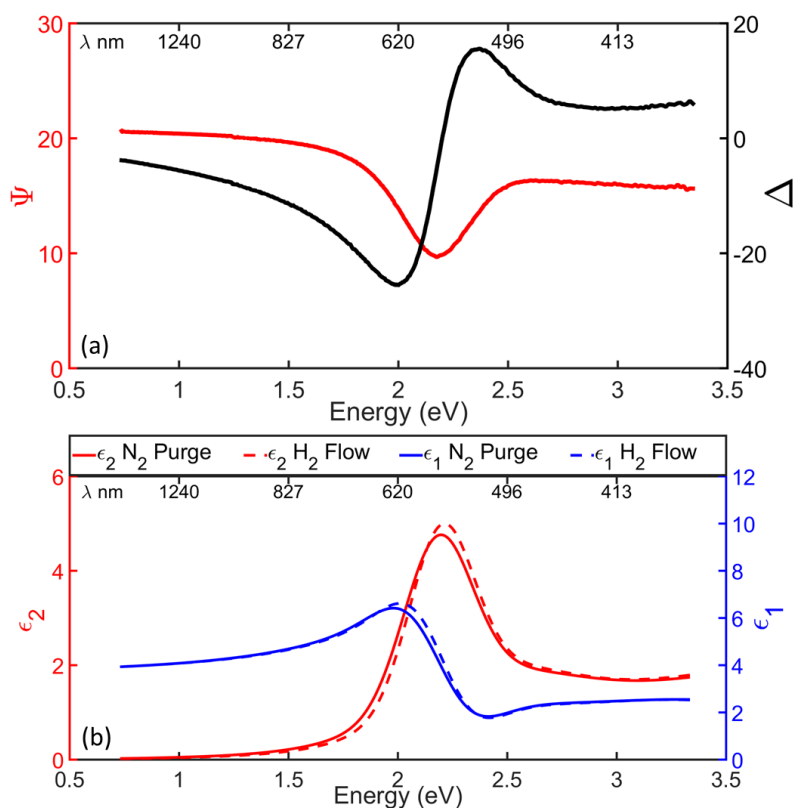


**Figure 1 Raw ellipsometry data and fit used to obtain the dielectric function. (a)** Raw ellipsometry data $\Psi$ (red) and $\Delta$ (black) as a function of frequency and wavelength for a film held under $N_2$ conditions. The fit cannot be distinguished from the data. **(b)** Real ($\varepsilon_1$, blue

curves) and imaginary ($\varepsilon_2$, red curves) parts of the dielectric function calculated based on the ellipsometry fits for samples held under $N_2$ (solid) and $H_2$ (dashed). All experiments carried out under broadband illumination.

Figure 1a illustrates raw ellipsometry data including the amplitude component ($\Psi$) and the phase difference ($\Delta$). The real ($\varepsilon_1$) and imaginary ($\varepsilon_2$) parts of the measured dielectric function are shown in Fig. 1b before and after exposure to $H_2$. The peak location in frequency of $\varepsilon_2$ was used to monitor changes in time of the film's surface. The time sequence of exposures to $N_2$ or $H_2$ is illustrated in Fig. 2a. The process can be divided into several steps. Initially, a dewetted gold nanoparticle sample, characterized by AFM[26] and shown in Fig. 2c, was exposed to nitrogen at 100 sccm under broadband illumination for 34 min.
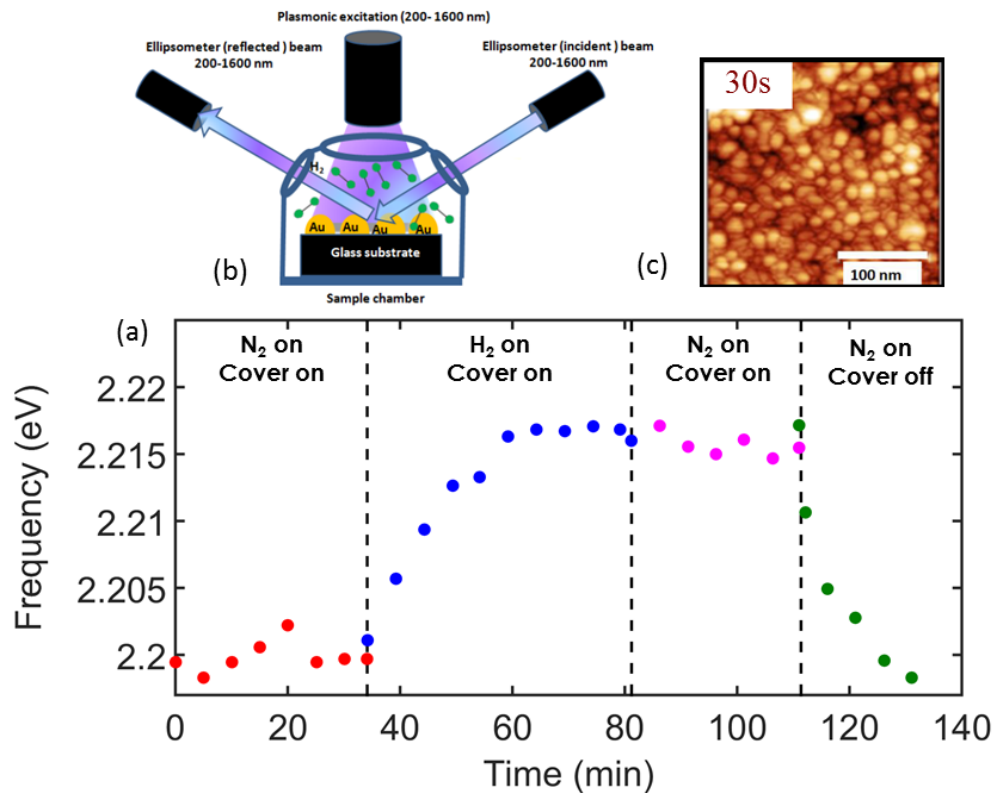
**Figure 2 Monitoring changes in the peak of the imaginary part of the dielectric function under $N_2$ and $H_2$ exposures. (a)** Time evolution of $\varepsilon_2$ peak location in frequency for gold nanoparticles. **(b)** Schematic of the *in situ* spectroscopic ellipsometry setup with broadband illumination from top. **(c)** AFM image of the 30 s sputtered dewetted gold nanoparticle thin-film sample showing particles of 10-20 nm size.

Then, the sample was exposed to a mixture of 95% nitrogen and 5% hydrogen (100 sccm) for 27 min, also under broadband illumination. During the $H_2$ flow, the $\varepsilon_2$ peak blue shifted from a frequency of 2.202 eV (563 nm) to 2.217 eV (559 nm) as shown in Fig. 1b. After hydrogen flow, nitrogen was turned on again for 30 min but recovery to the original state was not observed. Therefore, the top cover of the cell was taken off to further help purge the cell and nitrogen was kept on for an additional 35 min. This final step provided the recovery to the initial signal level. Clearly, an overall 0.02 eV blue shift in $\varepsilon_2$ was detected during $H_2$ exposure. Incidentally, a similar blue shift upon hydrogenation of gold nanoparticles in a $H_2$ electrical discharge was reported by Giangregorio *et al*.[2], and a blue shift in the LSPR of Au nanorods was observed in the presence of $H_2$ and Pt nanoparticles, presumably the source of atomic H by spillover.[27] Therefore, the presence of hydrogen significantly modifies the dielectric function, but nitrogen alone does not induce significant modifications. In fact, changes produced by nitrogen were smaller than 1% whereas the corresponding changes for hydrogen were as large as 4%. Moreover, switching the atmosphere from nitrogen to argon produced the same effect[26].

In order to interpret experimental results, guide analysis and serve as a baseline, first-principles, DFT-based calculations were performed to understand the interaction of gold surfaces with atomic H. For this purpose, we follow Norskov's[28] idea in considering a three-atomic-layer thick Au(111) slab with a H atom adsorbed at three different sites, namely, the bridge, the face

6

centered cubic (FCC), and the hexagonal close packed (HCP) site as illustrated in Fig. 3a. The Au(111) surface was relaxed within the GGA scheme and no significant surface reconstruction was found[29]. The potential energy (Fig. 3b) was computed for the surface and bulk of the gold unit cell. Moreover, a global minimum is exhibited at a height of 1 Å from the center of the top layer for the bridge site, while the corresponding global minima for FCC and HCP sites lie at 0.8 Å. The calculated binding energy, $E_b$=E(AuH)-E(Au)-E(H), of hydrogen in all three configurations was found to be 2.30 eV. We have further found that this binding energy is in good accord with the state-of-the-art strongly constrained and appropriately normed (SCAN) meta-GGA functional[30]. Such a value of binding energy is characteristic of chemisorption and is in agreement with previous results[31–33]. Furthermore, our results are consistent with Ref. [33] by Ferrin *et al.* which presents a comprehensive study of hydrogen adsorption, absorption and diffusion.
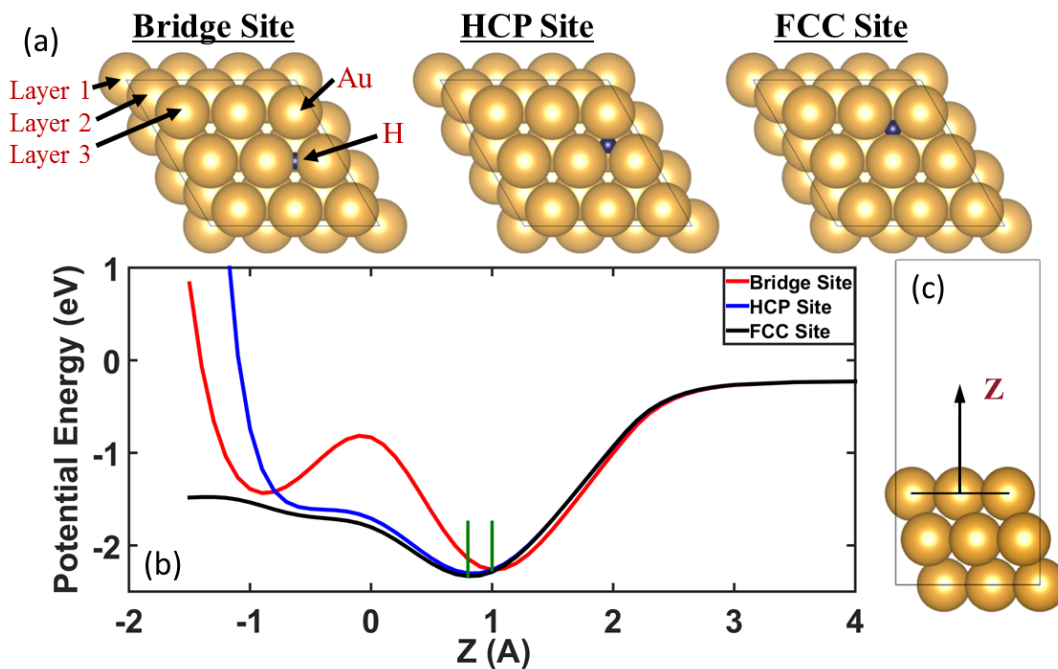


7

**Figure 3 DFT calculations simulating the interaction of atomic hydrogen with gold under optical illumination**. **(a)** Top view of three-atomic-layer Au(111) surface unit cell with a hydrogen atom (black) adsorbed at the bridge, hexagonal close packing, and face centered cubic sites, respectively. **(b)** Potential energy of a hydrogen atom for various adsorption sites as a function of the distance $z$ measured from the center of the top gold layer (right). **(c)** Z-axis overlaid on the side view of the unit cell, with zero measured from the center of the top layer. For scale, note that the radius of the gold atoms is 1.47 Å.

The prolonged robustness of the blue shift seen in Fig. 2a over the 80-110 min region is most striking. The fact that the cell cover needed to be removed for the system to recover indicates that only under exposure to other environmental species one can lift H off the gold surface. This observation allows us to infer that H-Au bonding at the surface is as favored as the formation of $H_2$. In fact, given that the binding energy of $H_2$ is 4.58 eV[34] within GGA, the activation energy for desorption is $E_a = E(H_2) - E(2H)_{surface} = 20$ meV which shows that surface adsorption is preferred, thermal fluctuations notwithstanding. Therefore, these arguments justify the absence of immediate recovery as shown in Fig. 2a indicating that a plasmonically driven gold hydride is formed and stabilized at the surface. Our results are also consistent with the desorption activation energies measured by Pan et al.[35]

To further elucidate the nature of the bond between hydrogen and gold, Fig. 4a shows the evolution of orbital occupation numbers of H as a function of the distance from the surface. A sharp transition is seen at approximately 2 Å bisecting two bonding regimes: covalent and van der Waals. In the covalent regime, at short distances from the gold surface, the populations of majority and minority occupied spin orbitals are equal and the electrons screening the proton have both $s$ and $p$ character. For distances greater than 2 Å, the screened proton essentially

becomes a hydrogen atom interacting with the gold surface via van der Waals forces. The potential minimum occurs at around 0.8 Å before the hydrogen atom is formed, so that the associated bond has a covalent rather than a van der Waals character. The sticking of the hydrogen at the surface may also be interpreted as a proton attracted by the electrostatic image potential produced by the metallic surface. Moreover, our computations show that the proton on the 3-layer Au(111) surface leads to substantial charge displacements and screening effects. These results are consistent with previous calculations by Takagi *et al.* [31] and by Wang *et al.*[32].
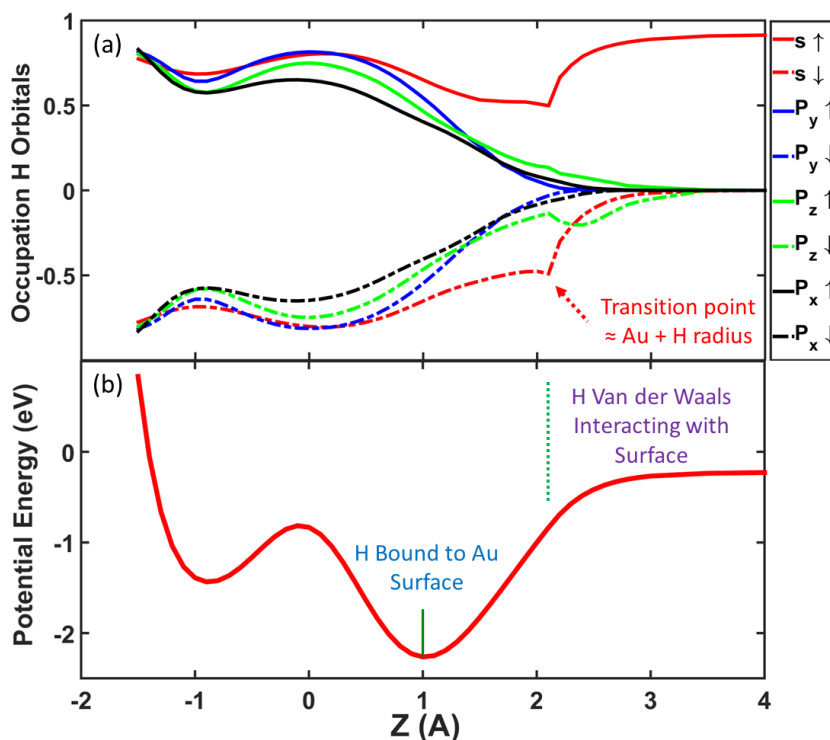


**Figure 4 Different regimes in the interaction between the gold surface and the hydrogen atom. (a)** H-atom orbital-projections as a function of height (Å) measured from the center of the top layer of the Au(111) surface. **(b)** Corresponding potential energy curve of hydrogen, where the transition at 2 Å is highlighted.

We simulated the effect of a thin gold hydride layer on the dielectric properties by placing an H atom at each of the three different available equilibrium sites. The dielectric function was obtained by calculating the imaginary part first as a joint-density-of-states with appropriate matrix elements. The real part was then obtained via a Kramers–Kronig transform. Dielectric function calculations were carried out using the Vienna *ab initio* simulation package (VASP) [36–38]. Results shown in Fig. 5 correspond to 11% H coverage. The peak of the imaginary part of the ZZ-component of the dielectric tensor is seen to undergo a larger blue shift of 0.06 eV compared to the observed value of 0.02 eV, indicating that H-coverage in the simulations is larger than in the experimentally measured sample. We have verified within our calculations that the blue-shift as a function of the H coverage follows a linear relationship up to saturation, therefore the observed experimental shift of 0.02 eV corresponds to 4% theoretical H coverage. Furthermore, our blue shift is in good accord with Collins *et al.*[27] and amplitude and lineshape of the calculated imaginary part of the dielectric function are also seen to agree remarkably well with the measurements of Giangregorio *et al.*[2]. Here, the differences with respect to Fig. 1b are attributed to deviations in the nanoparticle thin films from an Au(111) surface.
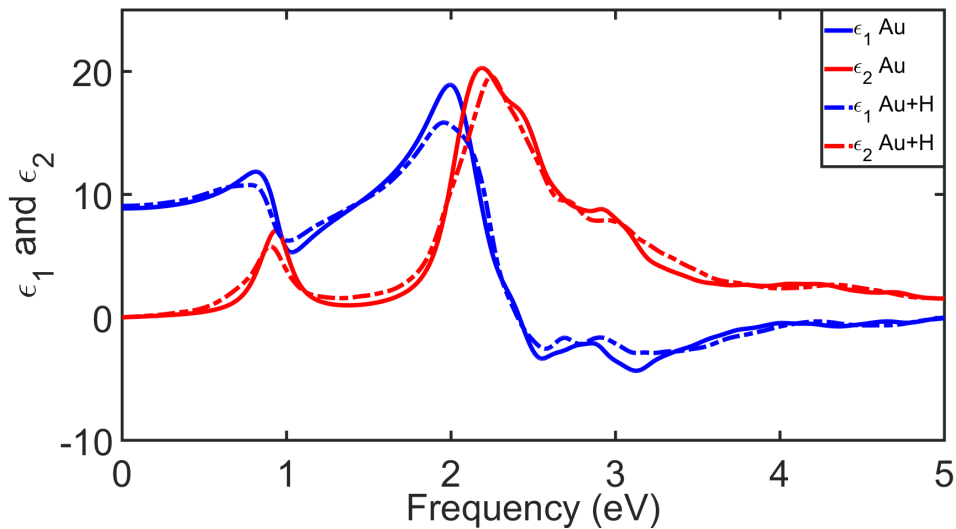
We now discuss the robustness of our blue shift findings. Previous rationalizations of the blue shift utilize a model dielectric function focusing on the Drude part and a well-defined charge transfer[2,24,25,39]. However, band structure contributions are vital for an accurate description of the optical properties of gold nano-structures[40] and the AuH bond exhibits strong covalent character[41]. Interestingly, small charge transfer has been found in the case of hydrides[41] while recent work on gold fluorides shows more significant charge transfer[42]. In the present case, the screening of a proton by the electron gas is important. In fact, our calculations indicate that about 0.05 electron per AuH bond are displaced by Friedel oscillations near the gold surface. Nevertheless, these Friedel charge redistributions cannot be associated with charge transfer. Therefore, our blue-shift is not produced by charge transfer but by the formation of the hydride leading to an enhancement of the critical band gaps in the electronic structure[40]. In conclusion, the correct blue-shift of the dielectric function can be explained only when full band structure and covalent bond formation are taken into account.

## Conclusion

We have shown that solids can be transformed into new materials via plasmonic excitations. We demonstrate this novel pathway for creating new materials by considering the formation of a metastable gold hydride layer through the dissociation of molecular hydrogen on films of gold nanoparticles. This reaction also drives changes in the dielectric constant and the

associated optical properties at the gold surface. Our study provides a new approach for exploring the bonding behavior between non-reactive noble metals and $H_2$ *in situ*, without the need for extreme experimental conditions[2,3], and opens up possibilities for novel methods of materials synthesis and low-concentration sensing applications. Clearly, our work shows that gold hydride should be considered as an intermediate in the crucial area of photocatalytic reactions such as the artificial photosynthesis of ammonia, which mitigates the high energy consumption of the Haber-Bosch process[43].

## Supplementary Information Summary

Details pertaining to sample preparation, ellipsometry measurements and density functional theory calculations are given.

## Acknowledgements

## Keywords

Ab initio calculations; Ellipsometry; Gold; Hydride

## Author Contributions

DS, CL, EG contributed equally to this work.

DS, EG, SS, ZF, and EB contributed towards the design and implementation of ellipsometry measurements and the interpretation of the results. KG, MH, and SN were responsible for the thin film preparation. CL, BB, RM and AB were responsible for the theoretical calculations and the interpretation of the results. All contributed to the writing of the manuscript.

## Competing Financial Interests

The authors declare no competing financial interests.

## References:

[1]    S. Mukherjee, F. Libisch, N. Large, O. Neumann, L. V. Brown, J. Cheng, J. B. Lassiter, E. A. Carter, P. Nordlander, N. J. Halas, *Nano Lett.* **2013**, *13*, 240–247.

[2]    M. M. Giangregorio, M. Losurdo, G. V. Bianco, A. Operamolla, E. Dilonardo, A. Sacchetti, P. Capezzuto, F. Babudri, G. Bruno, *J. Phys. Chem. C* **2011**, *115*, 19520–19528.

[3]    V. F. Degtyareva, *Journal of Alloys and Compounds* **2015**, *645*, *Supplement 1*, S128–S131.

[4]    S. Linic, P. Christopher, D. B. Ingram, *Nat Mater* **2011**, *10*, 911–921.

[5]    I. Thomann, B. A. Pinaud, Z. Chen, B. M. Clemens, T. F. Jaramillo, M. L. Brongersma, *Nano Lett.* **2011**, *11*, 3440–3446.

[6]    S. Mubeen, J. Lee, N. Singh, S. Krämer, G. D. Stucky, M. Moskovits, *Nat Nano* **2013**, *8*, 247–251.

[7]    J. W. Schwede, I. Bargatin, D. C. Riley, B. E. Hardin, S. J. Rosenthal, Y. Sun, F. Schmitt, P. Pianetta, R. T. Howe, Z.-X. Shen, et al., *Nat Mater* **2010**, *9*, 762–767.

[8]    J. R. Renzas, G. A. Somorjai, *J. Phys. Chem. C* **2010**, *114*, 17660–17664.

[9]    N. A. Joy, B. K. Janiszewski, S. Novak, T. W. Johnson, S.-H. Oh, A. Raghunathan, J. Hartley, M. A. Carpenter, *J. Phys. Chem. C* **2013**, *117*, 11718–11724.

[10]   M. Maillard, P. Huang, L. Brus, *Nano Lett.* **2003**, *3*, 1611–1615.

[11]   Y. Zhai, J. S. DuChene, Y.-C. Wang, J. Qiu, A. C. Johnston-Peck, B. You, W. Guo, B. DiCiaccio, K. Qian, E. W. Zhao, et al., *Nat Mater* **2016**, *15*, 889–895.

[12]   M. Murdoch, G. I. N. Waterhouse, M. A. Nadeem, J. B. Metson, M. A. Keane, R. F. Howe, J. Llorca, H. Idriss, *Nat Chem* **2011**, *3*, 489–492.

[13]   W. Hou, W. H. Hung, P. Pavaskar, A. Goeppert, M. Aykol, S. B. Cronin, *ACS Catal.* **2011**, *1*, 929–936.

[14]   D. Conklin, S. Nanayakkara, T.-H. Park, M. F. Lagadec, J. T. Stecher, X. Chen, M. J. Therien, D. A. Bonnell, *ACS Nano* **2013**, *7*, 4479–4486.

[15]   F. Wu, L. Tian, R. Kanjolia, S. Singamaneni, P. Banerjee, *ACS Appl. Mater. Interfaces* **2013**, *5*, 7693–7697.

[16]   Z. Gueroui, A. Libchaber, *Phys. Rev. Lett.* **2004**, *93*, 166108.

[17] L. Hayati, C. Lane, B. Barbiellini, A. Bansil, H. Mosallaei, *Phys. Rev. B* **2016**, *93*, 245411.

[18] B. Barbiellini, S. Das, V. Renugopalakrishnan, P. Somasundaran, *Condensed Matter* **2018**, *3*, 10.

[19] C. Li, Y. Zhang, M. T. Cole, S. G. Shivareddy, J. S. Barnard, W. Lei, B. Wang, D. Pribat, G. A. J. Amaratunga, W. I. Milne, *ACS Nano* **2012**, *6*, 3236–3242.

[20] D. Sil, K. D. Gilroy, A. Niaux, A. Boulesbaa, S. Neretina, E. Borguet, *ACS Nano* **2014**, *8*, 7755–7762.

[21] K. D. Gilroy, A. Sundar, M. Hajfathalian, A. Yaghoubzade, T. Tan, D. Sil, E. Borguet, R. A. Hughes, S. Neretina, *Nanoscale* **2015**, *7*, 6827–6835.

[22] I. P. Silverwood, S. M. Rogers, S. K. Callear, S. F. Parker, C. R. A. Catlow, *Chem. Commun.* **2016**, *52*, 533–536.

[23] T. Whittaker, K. B. S. Kumar, C. Peterson, M. N. Pollock, L. C. Grabow, B. D. Chandler, *J. Am. Chem. Soc.* **2018**, *140*, 16469–16487.

[24] R. Ishida, S. Yamazoe, K. Koyasu, T. Tsukuda, *Nanoscale* **2016**, *8*, 2544–2547.

[25] R. Ishida, S. Hayashi, S. Yamazoe, K. Kato, T. Tsukuda, *J. Phys. Chem. Lett.* **2017**, *8*, 2368–2372.

[26] D. Sil, *Synthesis and Applications of Plasmonic Nanostructures*, Temple University, **2015**.

[27] S. S. E. Collins, M. Cittadini, C. Pecharromán, A. Martucci, P. Mulvaney, *ACS Nano* **2015**, *9*, 7846–7856.

[28] B. Hammer, J. K. Nørskov, in (Ed.: B.-A. in Catalysis), Academic Press, **2000**, pp. 71–129.

[29] P. L. Hansen, J. B. Wagner, S. Helveg, J. R. Rostrup-Nielsen, B. S. Clausen, H. Topsøe, *Science* **2002**, *295*, 2053–2055.

[30] J. Sun, A. Ruzsinszky, J. P. Perdew, *Phys. Rev. Lett.* **2015**, *115*, 036402.

[31] S. Takagi, J. Hoshino, H. Tomono, K. Tsumuraya, *J. Phys. Soc. Jpn.* **2008**, *77*, 054705.

[32] S.-W. Wang, W. H. Weinberg, *Surface Science* **1978**, *77*, 14–28.

[33] P. Ferrin, S. Kandoi, A. U. Nilekar, M. Mavrikakis, *Surface Science* **2012**, *606*, 679–689.

[34] G. Kresse, J. Hafner, *Surface Science* **2000**, *459*, 287–302.

[35] M. Pan, A. J. Brush, Z. D. Pozun, H. Chul Ham, W.-Y. Yu, G. Henkelman, G. S. Hwang, C. Buddie Mullins, *Chemical Society Reviews* **2013**, *42*, 5002–5013.

[36] G. Kresse, J. Furthmüller, *Computational Materials Science* **1996**, *6*, 15–50.

[37] G. Kresse, J. Furthmüller, *Phys. Rev. B* **1996**, *54*, 11169–11186.

[38] M. Gajdoš, K. Hummer, G. Kresse, J. Furthmüller, F. Bechstedt, *Phys. Rev. B* **2006**, *73*, 045112.

[39] W. L. Watkins, Y. Borensztein, *Phys. Chem. Chem. Phys.* **2017**, *19*, 27397–27405.

[40] D. Rioux, S. Vallières, S. Besner, P. Muñoz, E. Mazur, M. Meunier, *Advanced Optical Materials* **2014**, *2*, 176–182.

[41] P. Pyykkö, *Angewandte Chemie International Edition* **2004**, *43*, 4412–4456.

[42] J. Lin, S. Zhang, W. Guan, G. Yang, Y. Ma, *J. Am. Chem. Soc.* **2018**, *140*, 9545–9550.

[43] T. Oshikiri, K. Ueno, H. Misawa, *Angew. Chem. Int. Ed.* **2016**, *55*, 3942–3946.

**Table of Contents Entry**

Localized surface plasmon resonances of metallic nanoparticles produce strong local field enhancements and offer unique processes to tailor light matter interactions at the nano scale. Such processes become all the more exciting as nanoparticles interact with molecules. The resulting hybrid system behaves differently from its constituent elements and yields novel optical properties. In this study, we combine first-principles simulations and in situ spectroscopic ellipsometry to show that a change in the optical properties (blue shift in the dielectric function) of gold nanostructures is justified by formation of gold hydride.